光学学报

面向散射光场调控的波前整形方法及其成像应用(特邀)

沈乐成[1]，罗嘉伟[2]，张志凌[1]，张诗按[1,3,4*]

[1]华东师范大学精密光谱科学与技术国家重点实验室，上海 200241；

[2]中山大学电子与信息工程学院，广东 广州 510006；

[3]山西大学极端光学协同创新中心，山西 太原 030006；

[4]华东师范大学-山东师范大学光场调控科学与光子芯片器件联合研究中心，华东师范大学精密光谱科学与技术国家重点实验室，上海 200241

摘要 光学散射一直以来都被认为是限制光学成像深度的重要因素。近年来，波前整形方法克服光学散射的能力引起了研究人员的广泛关注，其核心思想是通过对入射光进行相位调制，补偿散射引起的波前扰乱。波前整形方法能够有效地重新聚焦散射光，有望实现深层组织内高分辨率成像的目标。回顾了波前整形的历史发展，讨论了不同类型的波前整形方法，展示了其在克服光学散射以实现深层组织成像方面的应用实例，并展望了波前整形方法的未来发展趋势。

关键词 波前整形；散射介质；光学相位共轭；传输矩阵；光学成像；引导星

中图分类号 O438 **文献标志码** A **DOI**：10.3788/AOS231769

1 引 言

在当今众多成像应用中，光的传播通常受限于透明介质，如玻璃、空气和水。这些介质确保光在时域和空域的传播能够被准确地预测和调控，从而保障各类成像应用的顺利进行。然而，在实际应用中，光学散射会以随机方式改变光的传播方向，进而影响光路的可预测性，最终影响甚至破坏光学成像的效果。

生物组织中的光学散射现象主要源于微观折射率的不均匀性，这一长期存在的现象限制了光在生物组织中的成像深度[1]。如图 1(a)所示，光在生物组织中传播时将经历多次散射过程，其中，平均自由程(MFP)描述了光子在两次连续散射之间的平均传播距离，而传播平均自由程(TMFP)则表示光子在达到完全弥散状态前的平均传播距离。当光子的传播距离小于一个散射平均自由程时，其所在区域被称为“弹道光区域”，此时弹道光，即未经散射的光，占据主导地位。在可见光波段，生物软组织内的散射平均自由程约为 100 μm。传统光学显微镜依赖弹道光来实现成像，因此成像深度大多受限于 100 μm。在这种情况下，一些新型的光学成像方法，如光学相干断层成像[2]和多光子显微成像[3]，通过消除多次散射光的干扰来增加成像深度。然而，由于弹道光的强度随着成像深度的增加呈指数衰减，这些方法的成像深度仍然受到限制，通常在一个散射传播平均自由程内。在可见光波段，生物软组织的传播平均自由程约为 1 mm，这个深度通常被称为“弥散极限”[图 1(b)]，此时通过弹道光实现深层组织高分辨率成像几乎是不切实际的。另一方面，虽然计算成像能够通过数学物理建模利用多次散射光进行深层组织成像，但其计算负担巨大，而且所得图像的分辨率低至毫米或厘米量级，无法满足许多应用需求[4]。因此，在当前阶段，克服散射效应以实

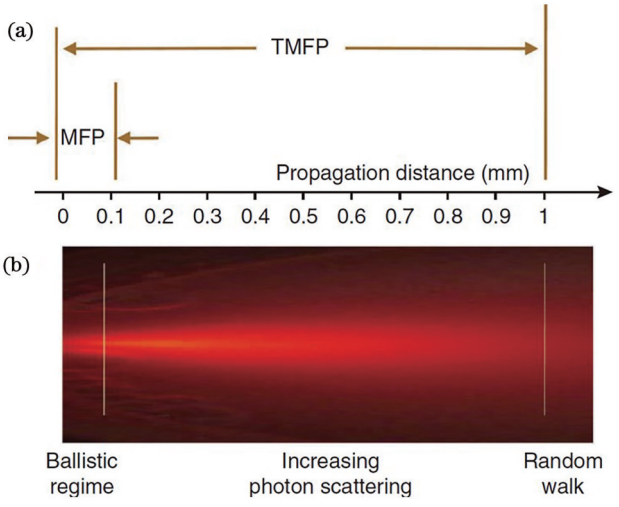

图 1 散射介质中光传播的示意图(以生物软组织为例)[1]

Fig. 1 Schematic illustration of light propagation in scattering media (using biological soft tissue as an example)[1]

收稿日期：2023-11-08；**修回日期**：2023-12-10；**录用日期**：2023-12-21；**网络首发日期**：2023-12-23

基金项目：国家自然科学基金(12004446，92150102，12325408，12274129)

通信作者：*sazhang@phy.ecnu.edu.cn

现深层组织的高分辨率光学成像仍然面临着巨大的挑战。

2 波前整形方法原理介绍

光学散射的随机性使得对散射光场的调控极具挑战。为了克服这一挑战，研究者们通过各种理论和实验手段探索和解析散射行为[5-15]。随着散射的深入研究，研究者们逐渐认识到在一定的时间尺度内，散射诱发的信息紊乱可以被视为一个确定性过程。通过对入射波前进行适当的预调制，散射效应引起的信息紊乱就可以得到有效恢复。在20世纪80年代，研究者们成功利用非线性光折变晶体开发了光学相位共轭方法。通过这一方法，他们有效地解决了多模光纤中类似于散射效应的模式串扰问题，并成功地通过多模光纤传输了清晰图像[16-17]。

随着微电子方法和材料科学的不断进步，空间光调制器（SLM）近年来备受研究者们的关注。SLM具有灵活且高效地调节光相位的能力，成为解决光学散射问题的有力工具。2007年，特温特大学的研究者们成功证明，即使经历了大量散射过程，相干光仍然可以通过特定的调制重新聚焦[18]。这一创新方法被命名为波前整形方法，为研究者们在穿透散射介质后进行高分辨率成像开辟了新的可能性。这一方法的推出不仅为实现生物体活体透明化提供了潜在路径，还为绕墙成像、穿云透雾、水下成像等[19-20]目标的实现注入了新的希望，其在科学研究和技术创新中的应用有望解决散射难题。波前整形方法的出现标志着光学成像领域迈出了重要的一步，为未来的探索和发展铺平了道路。

图2展示了基于波前整形实现散射光聚焦的原理。在图2（a）中，由于散射介质内折射率的不均匀性，未经调制的平面光穿过散射介质后在观测平面形成了随机的散斑图案。在数学上，线性的光学散射过程可以被认为是一个确定性的输入和输出过程，此时散射介质可以被建模为一个线性传输矩阵。在这个传输矩阵中，每个元素 t_{mn} 都是未知且随机的，它连接了入射光场的第 n 个元素与输出光场的第 m 个元素。由此可以将目标位置处的光场 E_m 表示为

$$E_m=\sum_{n=1}^{N}t_{mn}A_n\mathrm{e}^{\mathrm{i}\varphi_n},\tag{1}$$

式中：A_n 和 φ_n 分别代表入射光场第 n 个元素的幅值和相位；N 代表入射光场元素的数量。在入射光为平面波的情况下，可以简单假设 $A_n=1$ 和 $\varphi_n=0$。在上述传输矩阵中，每个元素 t_{mn} 是完全随机的，因此输出光场在不同位置处的分布呈现出散射光场随机叠加形成的散斑分布。在该物理模型下，实现特定位置输出光场的聚焦本质上就是实现目标位置 E_m 的光场振幅最大化。为了达到这个目标，贡献到 E_m 的各个组成复振幅元素必须是同相位的。为了在数学上满足该条件，可以简单地将入射相位 φ_n 设定为与 t_{mn} 的共轭相位相同。因此，波前整形方法的关键操作在于对入射光场进行预调制，进而在物理上实现所有相位的旋转和对齐，并最终实现目标光场振幅的最大化。如图2（b）所示，在采用波前整形方法之后，经过调制的光穿过散射介质后会形成一个明亮的焦点。

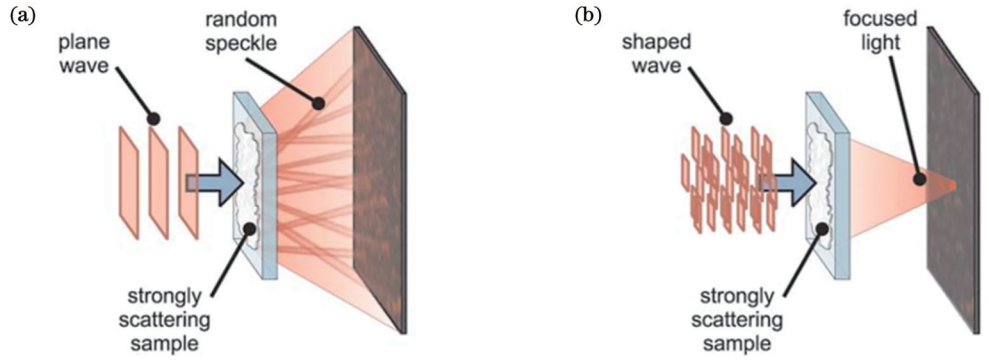

图2 通过透过散射介质实现光学聚焦的原理[18]。（a）平面波穿过散射介质后被散射，形成散斑图案；（b）被调制后的光场穿过相同散射介质后重新聚焦

Fig. 2 Principle of optical focusing through scattering media[18]. (a) Plane wave scatters after passing through scattering media, forming a speckle pattern; (b) modulated light field is refocused after passing through the same scattering media

波前整形方法通常采用基于液晶分子的SLM对入射波面进行纯相位调制，即只对相位 φ_n 进行调制而不对振幅 A_n 进行调制。理论证明，通过纯相位调制得到的增强因子可定义为调制后焦点光强与调制前散斑平均光强的比值[18]，可以表示为

$$\eta=\frac{\pi}{4}(N-1)+1,\tag{2}$$

式中：N 代表入射光场中可独立调控的模式数量。式（2）中的修正系数 $\pi/4$ 来源于非理想的纯相位调制，而在同时使用振幅和相位调制的理想调制情况下，该

系数应为1。除了采用纯相位调制外，SLM还可采用其他调制格式来实现波前整形，如二进制相位调制[21]、二进制振幅调制[22]和连续偏振调制[23]，这些调制格式引入的修正系数分别为1/π、1/π和0.394[21,24-27]。

在介绍了波前整形的基本原理后，接下来要讨论的是如何从实验上获取使得散射光聚焦的相位图。根据获取相位图信息的方式，波前整形方法的实现形式大体可以分为三类：基于反馈的波前整形、基于传输矩阵的波前整形和基于光学相位共轭的波前整形。在实现散射光聚焦的共同目标下，这三类波前整形方法获取的相位图是等效的，但是它们所对应的系统复杂度按前述顺序从简到繁。相应地，在获取相位图的效率上，这三类方法的算法复杂度从繁到简，时效性从高到低。

3 基于反馈的波前整形

首次实现散射光聚焦的方法是基于反馈的波前整形，该方法的系统搭建简单，复杂度较低。这种基于反馈的波前整形方法通过实时监测散射光的强度分布，利用反馈信号对波前进行优化，从而实现了散射光的再聚焦。这个系统的简易性和高效性使其成为初步研究和验证波前整形方法可行性的理想选择。图3展示了基于反馈的波前整形实现散射光再聚焦的系统装置[18]。该系统使用了波长为632.8 nm的激光器，发射出的红光经过SLM的相位调制后被聚焦到散射介质后方的平面。相机被用于实时监测目标平面上散射光的强度分布，为相位优化过程提供反馈信号。在这个实验中，研究者们选择了二氧化钛制备的散射样品进行测试。

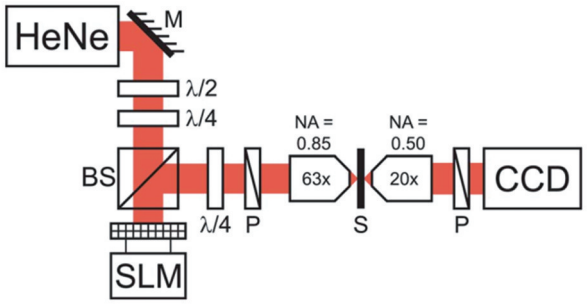

图3 基于反馈的波前整形实验装置示意图(HeNe为氦氖激光器，M为反射镜，λ/2为半波片，λ/4为四分之一波片，BS为50%非偏振分光镜，SLM为空间光调制器，P为偏振镜，S为散射介质，CCD为相机)[18]

Fig. 3 Schematic diagram of feedback-based wavefront shaping experimental setup (HeNe represents helium-neon laser, M represents mirror, λ/2 represents half-wave plate, λ/4 represents quarter-wave plate, BS represents 50% non-polarizing beam splitter, SLM represents spatial light modulator, P represents polarizing mirror, S represents scattering medium, and CCD represents camera)[18]

平面光直接穿透散射介质后，在目标位置形成了随机分布的散斑，如图4(a)所示。SLM的有效调控区域被划分为3228个独立区域，通过系统遍历SLM的每个独立区域，依次进行0～2π的相位循环检索后，研究者们逐步确定了最优相位图，以最大化目标位置的光强。将该相位图应用于入射光场的调控，实现了多条散射路径在目标位置的干涉相长，最终穿透散射介质实现光学聚焦。聚焦点的增强因子超过1000，如图4(b)所示。通过调整目标函数，研究者们还成功实现了散射光在多个目标位置的同时聚焦。图4(c)展示了5个增强因子超过200的光学焦点，其对应的调制相位分布如图4(d)所示。

图4的研究表明，经过特定调制的光场能够有效克服光学散射效应，从而穿过散射介质并实现光学聚焦和成像。该方法设计简洁，无需引入额外的参考光，在整个优化过程中能够保持较高的信噪比(SNR)。该方法基于目标位置强度反馈来寻找最佳相位分布，因此通常被称作基于反馈的波前整形方法。值得注意的是，基于反馈的波前整形的研究重点在于改进和升级贪婪算法以寻找最优相位分布。在文献[18]中使用的优化算法在初始迭代阶段容易受到测量噪声的影响。因此，为提高鲁棒性和收敛速度，已逐步研发和验证了一系列优化算法[22,28-39]。这些算法各有优劣，可根据实际应用需求在不同场合中进行选择[40]。举例来说，最早采用的逐步顺序算法(SSA)[18]和连续顺序算法(CSA)[28]在搜寻最优相位图的过程中收敛速度最快，且没有涉及任何冗余信息。然而，它们对噪声极为敏感，仅适用于信噪比特别高的一些应用场景。为解决这一问题，分区算法(PA)[28]和遗传算法(GA)[22,38]表现出极佳的抗噪声能力，但相应的代价是较慢的收敛速度，因此更适合噪声环境下的应用场景。另外，还存在一些相对折中的算法，例如哈达玛编码算法(HEA)[33,37]等，这些算法能够同时具备较强的鲁棒性和较快的收敛速度。此外，研究者们针对特殊应用，如时变环境等开发了一些智能优化算法[36,41-42]，这些算法在面对高于噪声水平的强扰动时表现出较高的适应性，有效避免了散射介质扰动导致的焦点强度衰减。

光束经波前整形后穿过散射介质，获得光学焦点后，可以通过扫描焦点的模式实现高分辨率成像。以光声成像为例，图5展示了对复杂结构的蜂翅膀进行成像的结果[43]。如图5(a)和(b)所示，当将该翅膀样品放置在散射介质后，无论是使用平面光照明还是使用随机散斑照明，都无法获得其结构的高分辨率图像。然而，当采用基于反馈的波前整形实现光学聚焦后，通过扫描光学焦点就能获得翅膀样品的高分辨率图像，获取如翅膀前缘大静脉和分支静脉交点等的丰富信息，如图5(c)所示。为了解决逐点扫描相对较慢的问题，研究者们还利用各种类型的记忆效应[44-45]，包括角度记忆效应[46-47]、平移记忆效应[48]、旋转记忆效应[49-51]

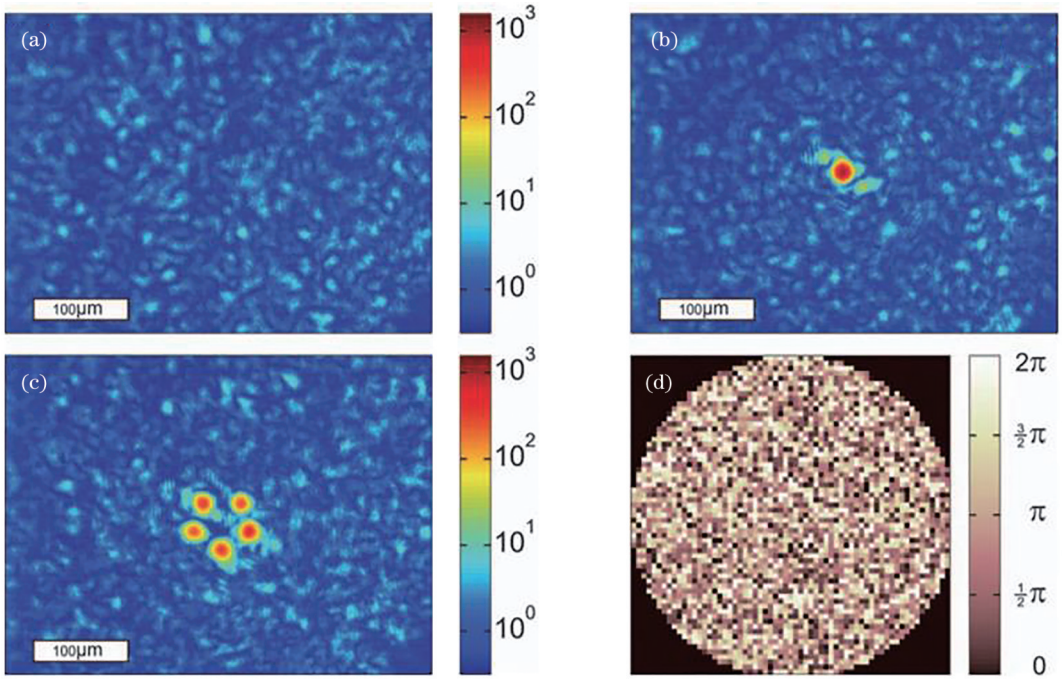

图 4 基于反馈的波前整形实现散射光聚焦的实验演示[18]。(a)平面光照明下的透射强度分布;(b)利用波前整形方法将散射光聚焦到单点,增强因子约为 1000;(c)利用波前整形方法将散射光聚焦到 5 个离散点,增强因子约为 200;(d)产生图 4(c)中结果所用的相位图

Fig. 4 Experimental demonstration of scattered light focusing using feedback-based wavefront shaping[18]. (a) Transmitted intensity distribution under plane wave illumination; (b) focusing scattered light to a single point using wavefront shaping, with an enhancement factor of approximately 1000; (c) focusing scattered light to five discrete points using wavefront shaping, with an enhancement factor of approximately 200; (d) phase map used to generate the result in Fig. 4(c)

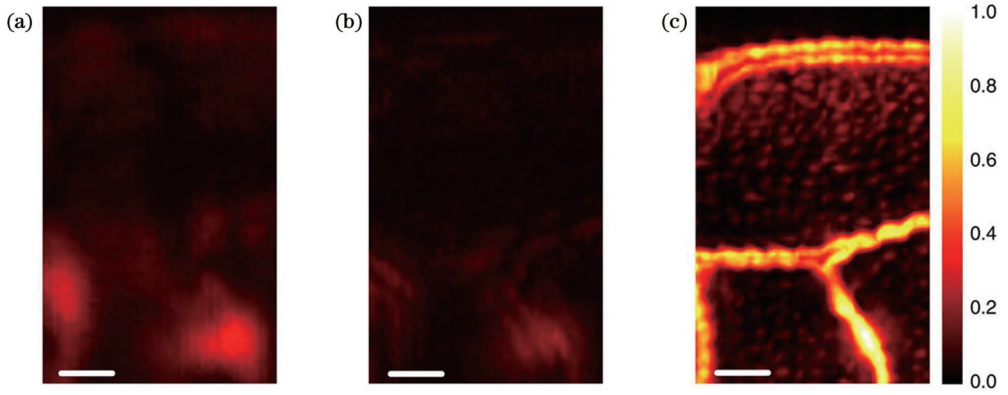

图 5 穿过散射介质对蜂翅膀进行成像的结果[43]。(a)均匀照明下的直接光声成像结果;(b)随机散斑照明下的直接光声成像结果;(c)通过波前整形优化后扫描焦点获得的高分辨率光声成像结果

Fig. 5 Imaging results of fly wings through scattering medium[43]. (a) Direct photoacoustic imaging result under uniform illumination; (b) direct photoacoustic imaging result under random speckle illumination; (c) high-resolution photoacoustic imaging result obtained by scanning focus point after optimization through wavefront shaping

以及光谱记忆效应[52-54]等,来提高光学焦点的扫描速度。

4 基于传输矩阵的波前整形

波前整形的核心思想是将光在散射介质中的传播过程建模为一个线性传输矩阵。因此,在完整获取了光学传输矩阵的信息后,便具备了穿过散射介质进行宽场成像的能力。首次基于传输矩阵的波前整形与宽场成像的实验演示对象是一个镀有(80 ± 25) μm 厚度的 ZnO 显微镜载玻片[55]。在该项研究中,传输矩阵连接了 SLM(输入)和相机(输出)平面,传输矩阵中的每个元素将这两个平面中的一对元素一一对应起来。通常来说,对该光学传输矩阵的测量需要得到输出面的复振幅光场,因此多引入参考光和全息光路。在该实验中,为了降低参考光束引入的相干噪声,研究者们使用了图 6 所示的共轴干涉方法。在具体实验方案中,

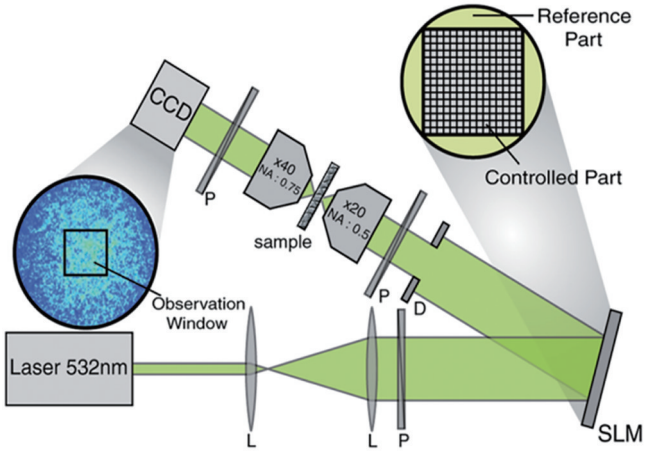

图 6 基于传输矩阵的波前整形实验装置示意图(L为透镜,SLM为空间光调制器,D为光阑,P为偏振片,CCD为相机)[55]

Fig. 6 Schematic diagram of the experimental setup for wavefront shaping based on the transmission matrix (L represents lens, SLM represents spatial light modulator, D represents aperture, P represents polarizer, CCD represents camera)[55]

输入光场中只有占SLM总有效面积65%的部分区域被调制,剩余占总有效面积35%的部分保持不变,作为静态参考光。值得注意的是,尽管该参考光在实验过程中保持不变,但其在相机的表面上呈现出随机的散斑分布,这造成了传输矩阵的每一行都附加了一个未知的复数因子。由于传输矩阵的每一行均独立进行干涉,这些复数因子的存在并不妨碍对散射光进行聚焦。

在实验中,传输矩阵的维度被设定为$N\times N$,其中$N=256$。此外,调控系统选择N个Hadamard基作为输入基底,结合四步相移的方法通过依次产生$4N$个相位图来获取$4N$个输出强度分布图。图7(a)展示了实验中相机测量到的一个散斑示例图像。研究者们基于矩阵理论,可以通过将加载模式与其对应的测量结果进行对应来构建传输矩阵。借助所获取的传输矩阵,研究者们便可方便地通过相位共轭将光聚焦至输出平面的任意位置。当SLM加载特定的共轭相位图时,一个明亮的焦点便显现于图7(b)中。为了展示该方法可实现输出平面任意位置的光学聚焦,图7(c)进一步展示了传输矩阵的归一化聚焦算符,其中较强的对角线元素验证了聚焦能力,而较弱的次对角线元素表明相邻像素间存在着一定的相关性。基于传输矩阵,图7(d)还展示了在三个不同位置上同时实现散射光场聚焦的能力。

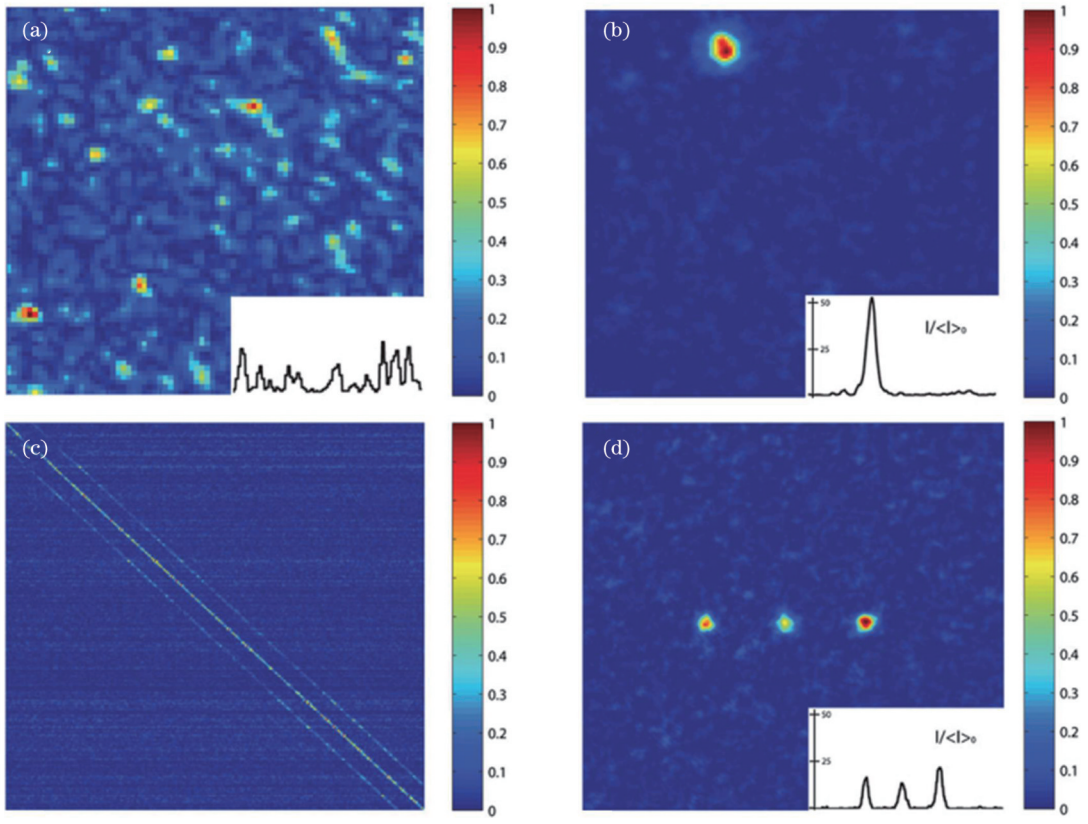

图 7 基于传输矩阵的波前整形方法实现散射光场聚焦的实验演示[55]。(a)平面波照明下的透射强度分布示例;(b)用波前整形方法将光聚焦到单个光点;(c)归一化聚焦算符;(d)用波前整形方法将光聚焦到三个离散光点

Fig. 7 Experimental demonstration of wavefront shaping based on the transmission matrix for focusing scattered light[55]. (a) Example of transmitted intensity distribution under plane wave illumination; (b) focusing light to a single point using wavefront shaping; (c) normalized focusing operator; (d) focusing light to three discrete points using wavefront shaping

在获取了散射介质传输矩阵的全部信息后，便可以其后方隐匿的物体进行宽场成像。数学上，隐匿物体的光场分布 $\boldsymbol{E}_{\text{in}}$ 能够通过输出光场 $\boldsymbol{E}_{\text{out}}$ 和传输矩阵 $\boldsymbol{T}$ 来进行推算，其计算表达式如下：

$$\boldsymbol{E}_{\text{in}} = \boldsymbol{T}^{\dagger}\boldsymbol{E}_{\text{out}}, \tag{3}$$

式中：算符 † 表示矩阵的转置共轭算符。式(3)的成立依赖于 $\boldsymbol{T}\boldsymbol{T}^{\dagger} \approx \boldsymbol{I}$ 的近似，这对于散射介质的传输矩阵通常是较为合理的。在测量噪声较低且传输矩阵的获取较为精准时，通过直接计算 $\boldsymbol{T}$ 的伪逆来重构物体图像是一种更好的选择[56]，该方法能够得到对比度更高的图像[57]。作为概念性验证，图 8 展示了利用式(3)对隐藏在散射介质后的物体进行重构后得到的图像。其中，图 8(a)和 8(b)分别展示了一个和两个物体的图像。该研究结果表明，不论散射介质引起的散射随机性如何，只需对散射介质的传输矩阵进行精准测量，即可实现对隐藏在其后方的物体进行宽场成像。这种宽场成像的方案较第 3 节中提到的点扫描方案效率更高。

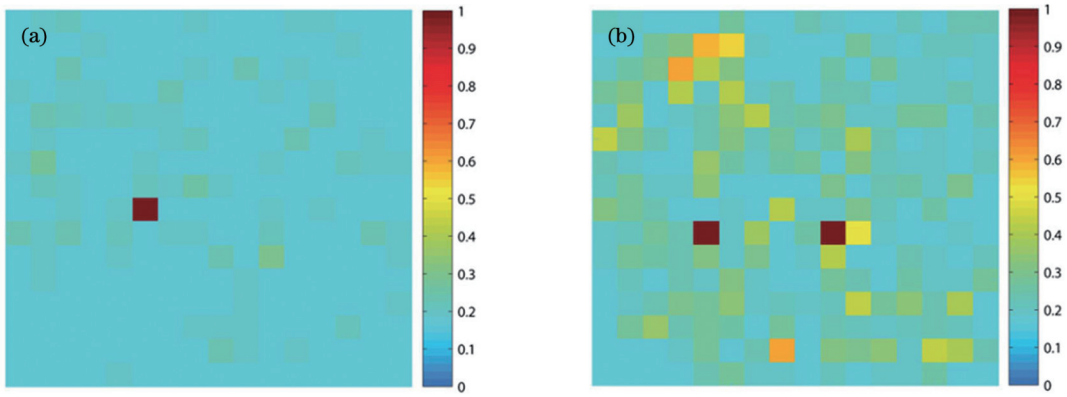

图 8 基于传输矩阵的波前整形对隐藏在散射介质后的物体进行宽场成像的实验结果[55]。(a)对一个物体进行成像；(b)对两个物体进行成像

Fig. 8 Experimental results of wide-field imaging of objects hidden behind scattering media using wavefront shaping based on transmission matrix[55]. (a) Image of a single object; (b) image of two objects

在众多测量散射介质传输矩阵的方法中，最直观且普遍应用的方法是采用外加参考光束的全息方法。该方法的主要优势在于它可以通过消除附加因子来实现对传输矩阵的精准重建，波前整形在全息成像[58]和时空成像[59-60]等领域的应用具有一定优势。然而，由于外加的参考光束对相干噪声非常敏感，另一种测量散射介质传输矩阵的方法是完全去除外部参考光束而采用基于相位恢复算法的直接强度检测。在该方法中，尽管实验装置简单且系统较为稳定，从强度信号中恢复振幅光场涉及到非线性方程组的求解，在没有适当约束的情况下存在多解性，且因易受局部最优值的干扰而无法收敛到最优结果。为了应对这一挑战，研究者们提出了多种相位恢复算法，并已在精确恢复散射介质的复振幅传输矩阵方面取得了卓越的成效[61-71]。其中，Gerchberg-Saxton(GS)算法是一种著名的相位恢复方法，能够通过快速迭代从一对关联的强度测量值中恢复出相位信息。通过适当改变该算法的迭代顺序，研究者们基于改进的 GS 算法对一根纤芯约为 50 μm、数值孔径约为 0.2、长度约为 1 m 的多模光纤的传输矩阵进行了高效并行测量[67]。在实验中，入射光调控的自由度控制在 400～600 之间，在使用 4 倍过采样率的条件下，传输矩阵的实验测量准确度约在 60%～70% 之间。利用测量的传输矩阵，研究者们进一步演示了穿过散射介质的单点和多点的高效聚焦。通过将反馈的理念引入 GS 迭代算法中，研究者们在保持重建结果准确度的情况下将过采样率进一步降低到了原来的 1/3，大幅减少了测量次数[68]。除此之外，将过采样率从时间维度拓展到空间维度也能够有效减少系统的测量次数，提高测量和调控的时效性[69]。这些成果为快速恢复大型光学传输矩阵提供了有效工具。

在一些特殊应用场景中，散射介质中存在着较强的非线性效应，在这种情况下，继续使用线性传输矩阵来描述散射过程变得不再合适，因此应引入更为复杂的张量描述方法[72-73]。随着近年来人工智能和计算算力的不断发展与提升，将非线性散射过程交给神经网络来处理成为了一种自然的选择。2018 年，深度学习首次被用来对经历过 1 km 长的多模光纤传输后已经完全变形扭曲的手写字母进行成功分类[74]。在该工作的启发下，神经网络随之被广泛地用于散斑成像，即从散射后测量到的散斑强度分布中恢复出原始图像[75-79]，其也被证实对于动态扰动下的多模光纤具有高鲁棒性的优点[80-82]。除了实现散斑成像，神经网络还可以用来穿过散射介质实现光学聚焦和图像投影[83-87]。这些结果都表明神经网络在操控非线性散射方面具有一定的优异性，可有效辅助波前整形应用于存在多模增益光纤和强吸收组织等的特定场景中。例如，在多模增益光纤中，由于无法使用线性传输矩阵建模，研究者们目前只能使用反馈的方法对输入光

场进行调控，实现输出光场脉冲形状、中心波长、时延等参数的灵活调控[88]。神经网络的强大能力将有望使得在非线性应用场景中对输出光参数的调控更为自如和高效，对新型激光的发展具有重要的价值。而在强吸收环境中，使用神经网络对非线性散射过程进行建模将有利于能量高效通道的探索[5-6, 89]，突破当前基于线性传输矩阵的方法遇到的实验瓶颈，对实现深层组织中的光学技术具有重要意义。即便是对于线性散射过程，近期的研究表明，神经网络也能与最大似然估计等方法结合，克服当前波前整形方法在依赖引导星、受控照明等方面的限制，针对特定的散射介质发展新型的成像技术[90]。

5 基于光学相位共轭的波前整形

基于反馈的波前整形方法通过迭代地执行优化算法来确定最优的相位图。在基于传输矩阵的波前整形方法中，构建传输矩阵的一个行向量需要遍历所有可能的输入模式。而基于神经网络的波前整形方法除了需要获取大量的训练集，还存在着一个耗时较长的训练过程。从这个角度看，这几种方法相对而言耗时较长，效率较低。基于光学相位共轭的波前整形方法仅需要单次测量即可确定传输矩阵的一个行向量，因此成为最高效的穿透散射介质聚焦的方法。该方法的核心物理机制在于光波传输方程的时间反演对称性。设想如图 9(a)所示的场景，其中入射光束从左向右传播进入散射介质而逐渐发散。假设时光倒流是可以实现的，那么这些发散的光束将会沿其先前的路径返回并恢复到原始状态。然而，在实际生活中时光倒流是无法实现的，幸运的是对于单频光而言，相位共轭可以模拟这种时间反演的效果。这意味着可以通过相位共轭来生成反射光束(即相位共轭光)，产生可以沿着之前路径返回至原始状态的光，这与时光倒流/时间反演的情形相似，如图 9(b)所示。

对于单频光，时间反演与光学相位共轭之间的等效性可以通过以下数学公式加以阐述。以一维平面波为例，沿 x 轴传播的光场 E_0 可表示为

$$E_0 = A\exp\left[\mathrm{i}\left(\omega t - kx + \varphi_0\right)\right], \tag{4}$$

式中：A 代表振幅；ω 代表角频率；k 和 φ_0 分别代表波矢大小和初始相位。式(4)描述了一个沿 $+x$ 方向传播的光。与此对应的时间反演光场同样满足波动方程，且可表示为

$$E_{\mathrm{TR}} = A\exp\left[\mathrm{i}\left(-\omega t - kx + \varphi_0\right)\right]。 \tag{5}$$

式(5)描述了沿 $-x$ 方向传播的光。将式(4)进行相位共轭，得到相位共轭光场 E_{OPC} 为

$$E_{\mathrm{OPC}} = A\exp\left[\mathrm{i}\left(\omega t + kx - \varphi_0\right)\right]。 \tag{6}$$

通过对比式(5)和(6)，可以看到二者均代表从右向左传播的光，且仅在相位上有一个负号的偏置。由于测量到的电场为复振幅的实数部分，因此时间反演和相位共轭在数学上完全等效，在实验中可以用相位共轭来等效地实现单色光的时间反演。基于该原因，有时候也把基于光学相位共轭的波前整形称为基于光学时间反演的波前整形。

在基于光学相位共轭的波前整形装置中，有两种不同的方法来实现相位共轭。第一种是基于光折变晶体的相位共轭镜，又称为模拟型相位共轭镜，在 20 世纪 80 年代，该方法被广泛用于解决多模光纤中的模式串扰问题[15-16]，2008 年研究者们进一步扩展了该方法的应用范围，利用它实现了穿透生物组织后的散射光聚焦[92]。该研究揭示了生物组织中散射效应的可补偿性，为波前整形在生物医学成像领域中的应用点亮了明灯。第二种实现光学相位共轭的方法是采用基于光电器件组合的数字型相位共轭镜。受益于近年来高速发展的微电子集成工艺，结合高性能相机和 SLM 的数字型相位共轭镜逐渐成为了主流方案。在此组合中，相机负责记录散射光场的信息，SLM 则生成对应的共轭光场。数字型光学相位共轭方法于 2010 年被提出[93]，其系统结构如图 10 所示，其中分光棱镜将相机

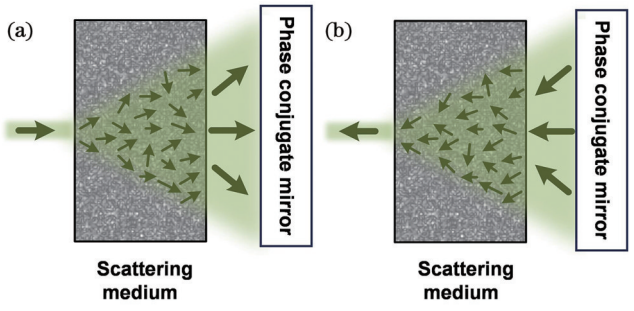

图 9 基于光学相位共轭的波前整形原理[91]。(a)前向散射过程；(b)相位共轭光的后向传播

Fig. 9 Principle of wavefront shaping based on optical phase conjugation[91]. (a) Forward scattering process; (b) backward propagation of phase-conjugated light

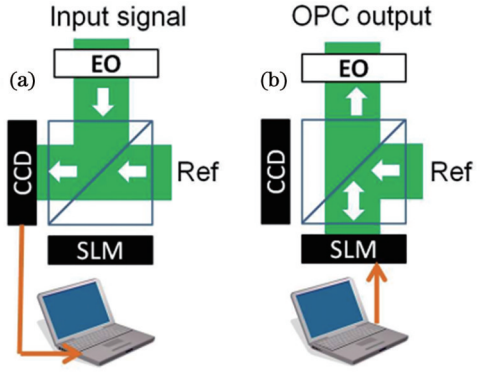

图 10 数字型光学相位共轭装置示意图[93]。(a)散射光场的测量步骤；(b)散射光场的调控步骤

Fig. 10 Schematic diagrams of digital optical phase conjugation device[93]. (a) Measurement steps of scattered light; (b) modulation steps of scattered light

与SLM置于光学对称平面上。基于相位共轭的波前整形主要包括两个步骤：散射光场测量步骤与散射光场调控步骤。如图 10(a)所示，分光棱镜在光场测量步骤中将输入散射光引向相机，结合参考光束实现散射光场的全息图像采集，并在计算机中进行数据处理以获取共轭相位图。在光场调控步骤中，SLM加载由计算机生成的共轭相位图，对入射平面光场进行相位调制，使其携带所需的共轭光场信息。如图 10(b)所示，被调制后的光场与原始的散射光产生时间反演的传播效果，该共轭光场穿过散射介质后就能有效地重现原先的光学焦点[21,24-27,51,91,94-100]。然而，需要注意的是，数字型光学相位共轭镜的工作原理是空间光调制器和相机处在完美的对称面，二者百万级的像素间也必须实现一一匹配，这在工程上实现起来非常麻烦。为了解决该工程问题，近年来研究者们提出了多种像素校准与匹配策略，以确保相机和SLM之间的像素能够实现一一对应[101-106]。图 10 中 EO 为电光相位调制器，Ref为参考光束。

相比较而言，模拟型光学相位共轭镜在处理速度和调控模式数上具有一定优势[107-110]，但其产生共轭波面的效率太低的问题造成其在应用中的适用性受到限制[111]。此外，这种基于光折变晶体的模拟型光学共轭方法对系统中波长的选择和功率的变化极为敏感，也不利于应用的开展。与之对应的是，数字型光学相位共轭镜在调制效率和波长不敏感方面占据优势，使得其在光学成像、调控、治疗等应用场景中占据了优势。总体来说，相比于前述的两种波前整形方法，基于光学相位共轭的波前整形能够高效地获取散射光场信息、调控散射光场，在面向动态散射过程的应用场景中极具优势[21,24,97,98]。

以活体组织内的成像应用为例，血液流动、心脏跳动、呼吸起伏等生理过程使得光学散射处于一个动态环境，散斑相关时间在毫秒乃至亚毫秒内[110]。波前整形的工作原理基于一个确定性的散射过程，因而要求散射光场的测量和调控在散射过程发生变化前即散斑相关时间内完成。因此，散射光场调控中的平均每模式时间就显得格外重要。该参数描述了调控系统中平均每个独立调控模式所消耗的时间，用散射样品的相关时间除以平均每模式时间可以得出在散射过程发生变化前，系统所能调控的最大独立模式数[100]。基于反馈的波前整形方法受限于反馈机制和优化算法效率最低，即使是当前最快的系统，其平均每模式时间也在百微秒量级[112]。基于传输矩阵的波前整形方法避免了反馈耗时，通过与声光调制编码方案结合，目前的平均每模式时间能够缩短到 1 μs 左右[52]。基于光学相位共轭的波前整形方法拥有最短的平均每模式时间，平均每模式时间可减小到百纳秒内[21]。近期，研究者们结合空间四分相位编码方案，实现了短至 29 ns 的平均每模式时间，并用该高速调控系统穿透约 5 mm 厚的成年活体斑马鱼进行了内部聚焦演示[100]。基于这些情况，基于光学相位共轭的波前整形是目前最有希望被应用于活体深层高分辨成像的方法。

6 用于辅助散射介质内聚焦的引导星

前面讨论的所有波前整形方法都有一个共同的目标，即穿过散射介质对散射光进行聚焦和成像。为了实现该目标，通常需要访问散射介质的另一侧，例如预先放置相机和单像素探测器。然而，在绝大部分的应用场景中，特别是深层组织的生物医学成像中，这种访问散射介质另一侧的情况往往是不存在的。因此，波前整形方法需要与适当的引导星相结合以实现散射介质内部的聚焦和成像。散射介质内的引导星通过与散射光产生局部相互作用，产生强度、相位乃至频率上可观测的变化[113]。波前整形通过感知这些变化来定位引导星的位置，进而引导散射光在引导星的位置处实现聚焦。值得注意的是，引导星的各种属性，例如它的大小以及产生变化的对比度，都将直接决定光学焦点的大小和亮度。

目前已开展的研究工作展示了多种类型的物理引导星，其中包括荧光分子[95,114-115]、二次谐波纳米粒子[94,116]、磁性粒子[117-118]、微气泡[119]及基因编码的荧光蛋白[120]。这些引导星由于其较小的尺寸和较高的对比度，能产生小而亮的光学焦点。但是，这些引导星仍然存在着一定的侵入性，并且一旦放置在生物组织内就难以自由移动。除此之外，生物组织内可产生的吸收变化的内源性散射体也可以作为非侵入性的引导星[121-122]，然而它们在生物组织内常常成片出现且难于操纵，因此也不是理想的选择。

相对于上述的物理引导星，聚焦的超声波提供了一种“虚拟引导星”，它在生物组织内部的位置可以随意调整。该引导星于 2011 年被首次提出并被应用在基于光学相位共轭的波前整形中，成功地实现了散射介质内的光学聚焦和成像[109]。图 11 描述了使用聚焦超声波作为引导星的工作机制。超声波相比于光在生物组织中具有更好的穿透特性，因此可以在组织内部产生一个较小的声学聚焦区域。在图 11(a)的散射光场测量步骤中，声光相互作用会使得超声聚焦区域内的部分光发生等量超声频率的频率偏移，这部分光被标记为“频移光”，通过光学相干的手段可将其与其他未标记的光进行分离。如图 11(b)所示，只对这些被标记的光进行光学相位共轭就能使得它们追踪原始路径并回到原先超声波聚焦的位置。这意味着在光学散射的影响下，研究者们能够在聚焦超声波的引导下在散射介质内实现一个明亮的光学焦点。通过对这个焦点进行扫描并测量频移光的强度，研究者们就能够重建散射介质内部物体的吸收分布图像[109]。

此外，两个美国的研究团队分别独立地证明了结合超声波引导星的光学聚焦方法，能够在深层散射介

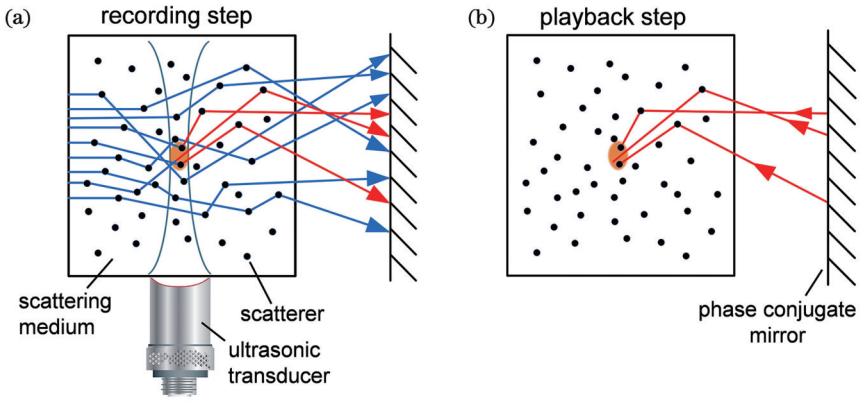

图 11 利用超声波引导星在散射介质内部聚焦光的工作原理。(a)在光场测量步骤中,通过频率选择只测量被超声标记的光场;(b)在光场调控步骤中,光学相位共轭只应用于被标记光的光场

Fig. 11 Principle of focusing light inside a scattering medium using ultrasonic guided stars. (a) In the wavefront measurement step, only the light tagged by ultrasound is measured through frequency selection; (b) in the wavefront modulation step, optical phase conjugation is applied only to the light tagged by ultrasound

质中实现荧光成像[123-124],这些成像结果展示在图 12 中。如图 12(a)所示,荧光成像目标夹在两片厚度为 2.5 mm 的鸡胸肉组织之间,成像系统中的超声换能器协助散射光在散射介质内部聚焦。图 12(b)呈现了未嵌入组织前的清晰荧光图像,图 12(c)展示了荧光目标嵌入散射介质后观察得到的模糊图像。作为对比,图 12(d)显示了采用波前整形方法后通过点扫描方法获得的清晰荧光图像。此外,图 12(e)~(g)还展示了嵌入组织中的肿瘤微组织的荧光成像结果。这些发现突显了结合了超声引导星的波前整形在克服复杂散射、实现散射组织内部荧光成像方面表现出的优越性能。

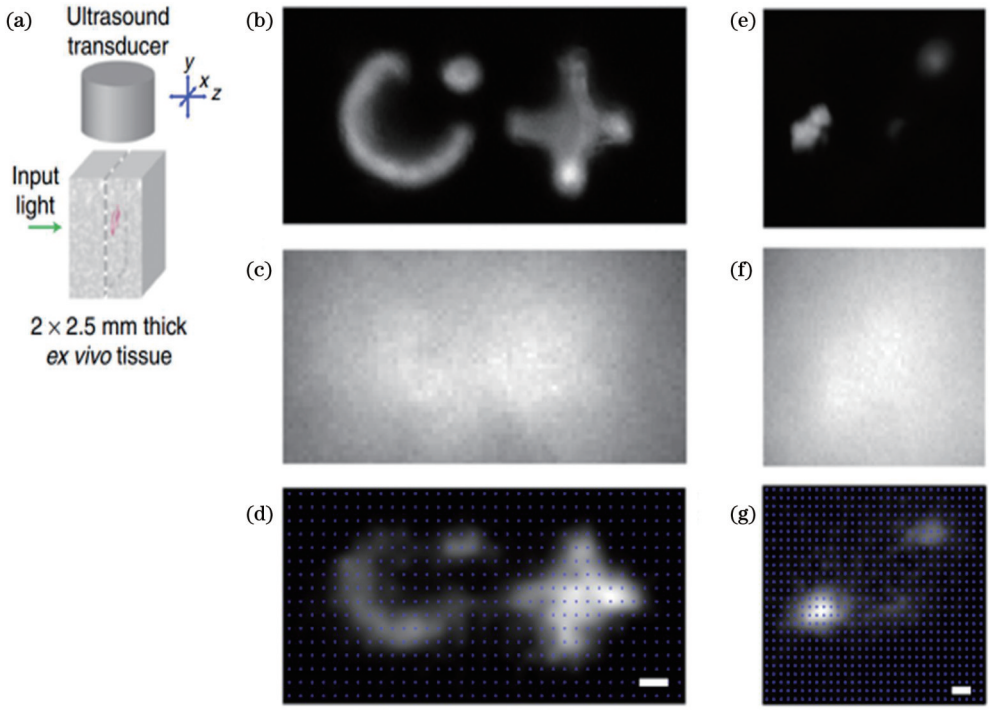

图 12 结合超声引导星的数字型光学相位共轭方法实现散射介质内的荧光成像[123]。(a)成像示意图;(b)嵌入散射介质前的清晰图像;(c)嵌入散射介质后的直接成像结果,其特征变得无法分辨;(d)波前整形后的点扫描成像结果;(e)包埋前肿瘤微组织的清晰图像;(f)包埋后肿瘤微组织的直接成像结果;(g)波前整形后的点扫描肿瘤微组织成像结果

Fig. 12 Digital optical phase conjugation method combining ultrasonic guided stars used for fluorescence imaging in scattering media[123]. (a) Schematic of the imaging process; (b) clear image before embedding in the scattering medium; (c) direct imaging result after embedding in the scattering medium, where features become indistinguishable; (d) point scanning imaging result after wavefront shaping; (e) clear image of the tumor before embedding; (f) direct imaging result of the tumor after embedding; (g) point scanning imaging result of the tumor after wavefront shaping

在上述成像系统中，成像分辨率受超声波焦点大小的限制，被超声波的衍射极限限制在数十到数百微米之间。这一分辨率对于大多数生物组织的成像是不够的。为了应对这一挑战，研究者们提出将光学相位共轭方法进行数次迭代，成功地缩小焦点尺寸并增强焦点光强[106,125-126]。研究者们还发现，这一方法不仅可以通过硬件实现，还可以通过计算方法进行[127]，同时还能加快点扫描的速度[128]。考虑到测量噪声和潜在的系统误差，已报道的实验优化结果在分辨率上提高了2～3倍，在焦点光强上提高了20倍[125]。除了采用迭代方法，研究者们还尝试利用散斑强度的涨落方差对散射光进行编码处理，以突破超声波的衍射极限并获得小至5 μm的光学焦点。然而，该方法需要进行数千次的统计测量过程，耗时较长[129]。

此外，研究者们对光声效应作为一种独特的虚拟引导星也表现出浓厚兴趣。例如，在基于反馈的波前整形研究中，光声信号可作为优化算法的一种反馈手段[43,130-133]；而在基于传输矩阵的波前整形研究中，研究者们可以直接测量光声传输矩阵，从而在散射介质深处实现光声成像[134-135]。总而言之，为了在无法直接访问的散射介质内部实现聚焦和成像，开发小体积、高对比度、非侵入性、易操控的引导星成为了当下波前整形的研究热点。

7 总　　结

近年来，半导体制造技术、计算资源和信息理论的扩展为计算光学成像带来了新的机遇，使得研究人员能够获取振幅、相位、偏振和角动量等多维光场信息。然而，在实际应用中，任何新型的光学成像模态的成像深度均受到光学散射的制约。波前整形提供了一个有效的调控手段，通过深入研究光学散射以及精确地控制大规模的散射光场，可消除散射带来的信息紊乱，实现散射介质中的高分辨率光学成像。目前，波前整形已成为一个跨学科的研究热点，其发展依赖于新方法和新理论的支持。然而，受限于现有光电设备的响应带宽以及重建算法的效率，目前波前整形在处理动态散射过程中仍面临着技术挑战，尤其是在面向生物活体、流动的浑浊水体或空气湍流等场景时，仍然无法较好地完成实时调控与成像[24,52,98,112,136]。同时，对于表现出非线性特性的复杂系统，波前整形的理论框架仍有待进一步明确和完善。尽管如此，我们仍然对波前整形的未来充满期待，相信其巨大的潜力会为散射介质内部的高分辨率成像等多种应用场景带来巨大的价值。

参 考 文 献

[1] Ntziachristos V. Going deeper than microscopy: the optical imaging frontier in biology[J]. Nature Methods, 2010, 7: 603-614.

[2] Huang D, Swanson E A, Lin C P, et al. Optical coherence tomography[J]. Science, 1991, 254(5035): 1178-1181.

[3] Helmchen F, Denk W. Deep tissue two-photon microscopy[J]. Nature Methods, 2005, 2(12): 932-940.

[4] Chance B, Kang K, He L, et al. Highly sensitive object location in tissue models with linear in-phase and anti-phase multi-element optical arrays in one and two dimensions[J]. Proceedings of the National Academy of Sciences, 1993, 90(8): 3423-3427.

[5] Vellekoop I M, Mosk A P. Universal optimal transmission of light through disordered materials[J]. Physical Review Letters, 2008, 101(12): 120601.

[6] Choi W, Mosk A P, Park Q H, et al. Transmission eigenchannels in a disordered medium[J]. Physical Review B, 2011, 83(13): 134207.

[7] Chong Y D, Stone A D. Hidden black: coherent enhancement of absorption in strongly scattering media[J]. Physical Review Letters, 2011, 107(16): 163901.

[8] Goetschy A, Stone A D. Filtering random matrices: the effect of incomplete channel control in multiple scattering[J]. Physical Review Letters, 2013, 111(6): 063901.

[9] Liew S F, Popoff S M, Mosk A P, et al. Transmission channels for light in absorbing random media: from diffusive to ballistic-like transport[J]. Physical Review B, 2014, 89(22): 224202.

[10] Popoff S M, Goetschy A, Liew S F, et al. Coherent control of total transmission of light through disordered media[J]. Physical Review Letters, 2014, 112(13): 133903.

[11] Kim M, Choi W, Yoon C Y, et al. Exploring anti-reflection modes in disordered media[J]. Optics Express, 2015, 23(10): 12740-12749.

[12] Liew S F, Cao H. Modification of light transmission channels by inhomogeneous absorption in random media[J]. Optics Express, 2015, 23(9): 11043-11053.

[13] Hsu C W, Goetschy A, Bromberg Y, et al. Broadband coherent enhancement of transmission and absorption in disordered media [J]. Physical Review Letters, 2015, 115(22): 223901.

[14] Yamilov A, Petrenko S, Sarma R, et al. Shape dependence of transmission, reflection, and absorption eigenvalue densities in disordered waveguides with dissipation[J]. Physical Review B, 2016, 93(10): 100201.

[15] He Y, Wu D X, Zhang R S, et al. Genetic-algorithm-assisted coherent enhancement absorption in scattering media by exploiting transmission and reflection matrices[J]. Optics Express, 2021, 29(13): 20353-20369.

[16] Beckwith P H, McMichael I, Yeh P. Image distortion in multimode fibers and restoration by polarization-preserving phase conjugation[J]. Optics Letters, 1987, 12(7): 510-512.

[17] McMichael I, Yeh P, Beckwith P. Correction of polarization and modal scrambling in multimode fibers by phase conjugation [J]. Optics Letters, 1987, 12(7): 507-509.

[18] Vellekoop I M, Mosk A P. Focusing coherent light through opaque strongly scattering media[J]. Optics Letters, 2007, 32 (16): 2309-2311.

[19] Cao R Z, de Goumoens F, Blochet B, et al. High-resolution non-line-of-sight imaging employing active focusing[J]. Nature Photonics, 2022, 16: 462-468.

[20] Zhu Y M, Zeng T J, Liu K W, et al. Full scene underwater imaging with polarization and an untrained network[J]. Optics Express, 2021, 29(25): 41865-41881.

[21] Liu Y, Ma C, Shen Y C, et al. Focusing light inside dynamic scattering media with millisecond digital optical phase conjugation[J]. Optica, 2017, 4(2): 280-288.

[22] Conkey D B, Brown A N, Caravaca-Aguirre A M, et al. Genetic algorithm optimization for focusing through turbid media in noisy environments[J]. Optics Express, 2012, 20(5): 4840-4849.

[23] Park J, Park J H, Yu H, et al. Focusing through turbid media

by polarization modulation[J]. Optics Letters, 2015, 40(8): 1667-1670.
[24] Wang D F, Zhou E H, Brake J, et al. Focusing through dynamic tissue with millisecond digital optical phase conjugation [J]. Optica, 2015, 2(8): 728-735.
[25] Shen Y C, Liu Y, Ma C, et al. Focusing light through scattering media by full-polarization digital optical phase conjugation[J]. Optics Letters, 2016, 41(6): 1130-1133.
[26] Shen Y C, Liu Y, Ma C, et al. Sub-Nyquist sampling boosts targeted light transport through opaque scattering media[J]. Optica, 2017, 4(1): 97-102.
[27] Yang J M, Shen Y C, Liu Y, et al. Focusing light through scattering media by polarization modulation based generalized digital optical phase conjugation[J]. Applied Physics Letters, 2017, 111(20): 201108.
[28] Vellekoop I M, Mosk A P. Phase control algorithms for focusing light through turbid media[J]. Optics Communications, 2008, 281(11): 3071-3080.
[29] Huang H L, Chen Z Y, Sun C Z, et al. Light focusing through scattering media by particle swarm optimization[J]. Chinese Physics Letters, 2015, 32(10): 104202.
[30] Fang L J, Zuo H Y, Yang Z G, et al. Particle swarm optimization to focus coherent light through disordered media[J]. Applied Physics B, 2018, 124(8): 155.
[31] Fang L J, Zhang X C, Zuo H Y, et al. Focusing light through random scattering media by four-element division algorithm[J]. Optics Communications, 2018, 407: 301-310.
[32] Wu Y L, Zhang X D, Yan H M. Focusing light through scattering media using the harmony search algorithm for phase optimization of wavefront shaping[J]. Optik, 2018, 158: 558-564.
[33] Wu Z H, Luo J W, Feng Y H, et al. Controlling 1550-nm light through a multimode fiber using a Hadamard encoding algorithm [J]. Optics Express, 2019, 27(4): 5570-5580.
[34] Wu D X, Qin L X, Luo J W, et al. Delivering targeted color light through a multimode fiber by field synthesis[J]. Optics Express, 2020, 28(13): 19700-19710.
[35] Zhao Y Y, He Q Z, Li S N, et al. Gradient-assisted focusing light through scattering media[J]. Optics Letters, 2021, 46(7): 1518-1521.
[36] Woo C M, Li H H, Zhao Q, et al. Dynamic mutation enhanced particle swarm optimization for optical wavefront shaping[J]. Optics Express, 2021, 29(12): 18420-18426.
[37] Luo J W, Wu Z H, Wu D X, et al. Efficient glare suppression with Hadamard-encoding-algorithm-based wavefront shaping[J]. Optics Letters, 2019, 44(16): 4067-4070.
[38] Wu D X, Luo J W, Li Z H, et al. A thorough study on genetic algorithms in feedback-based wavefront shaping[J]. Journal of Innovative Optical Health Sciences, 2019, 12(4): 1942004.
[39] Luo J W, Liang J J, Wu D X, et al. Simultaneous dual-channel data transmission through a multimode fiber via wavefront shaping[J]. Applied Physics Letters, 2023, 123(15): 151106.
[40] Vellekoop I M. Feedback-based wavefront shaping[J]. Optics Express, 2015, 23(9): 12189-12206.
[41] Yang Z G, Fang L J, Zhang X C, et al. Controlling a scattered field output of light passing through turbid medium using an improved ant colony optimization algorithm[J]. Optics and Lasers in Engineering, 2021, 144: 106646.
[42] Li H H, Woo C M, Zhong T T, et al. Adaptive optical focusing through perturbed scattering media with a dynamic mutation algorithm[J]. Photonics Research, 2021, 9(2): 202-212.
[43] Conkey D B, Caravaca-Aguirre A M, Dove J D, et al. Super-resolution photoacoustic imaging through a scattering wall[J]. Nature Communications, 2015, 6: 7902.
[44] Osnabrugge G, Horstmeyer R, Papadopoulos I N, et al. Generalized optical memory effect[J]. Optica, 2017, 4(8): 886-892.
[45] Liu H L, Liu Z T, Chen M J, et al. Physical picture of the optical memory effect[J]. Photonics Research, 2019, 7(11): 1323-1330.
[46] Feng S, Kane C, Lee P A, et al. Correlations and fluctuations of coherent wave transmission through disordered media[J]. Physical Review Letters, 1988, 61(7): 834-837.
[47] Schott S, Bertolotti J, Léger J F, et al. Characterization of the angular memory effect of scattered light in biological tissues[J]. Optics Express, 2015, 23(10): 13505-13516.
[48] Judkewitz B, Horstmeyer R, Vellekoop I M, et al. Translation correlations in anisotropically scattering media[J]. Nature Physics, 2015, 11: 684-689.
[49] Wang C, Ji N. Characterization and improvement of three-dimensional imaging performance of GRIN-lens-based two-photon fluorescence endomicroscopes with adaptive optics[J]. Optics Express, 2013, 21(22): 27142-27154.
[50] Amitonova L V, Mosk A P, Pinkse P W H. Rotational memory effect of a multimode fiber[J]. Optics Express, 2015, 23(16): 20569-20575.
[51] Ma C J, Di J L, Li Y, et al. Rotational scanning and multiple-spot focusing through a multimode fiber based on digital optical phase conjugation[J]. Applied Physics Express, 2018, 11(6): 062501.
[52] Wei X M, Shen Y C, Jing J C, et al. Real-time frequency-encoded spatiotemporal focusing through scattering media using a programmable 2D ultrafine optical frequency comb[J]. Science Advances, 2020, 6(8): eaay1192.
[53] Zhu L D, de Monvel J B, Berto P, et al. Chromato-axial memory effect through a forward-scattering slab[J]. Optica, 2020, 7(4): 338-345.
[54] Zhang R S, Du J Y, He Y, et al. Characterization of the spectral memory effect of scattering media[J]. Optics Express, 2021, 29(17): 26944-26954.
[55] Popoff S M, Lerosey G, Carminati R, et al. Measuring the transmission matrix in optics: an approach to the study and control of light propagation in disordered media[J]. Physical Review Letters, 2010, 104(10): 100601.
[56] Popoff S M, Lerosey G, Fink M, et al. Controlling light through optical disordered media: transmission matrix approach [J]. New Journal of Physics, 2011, 13(12): 123021.
[57] Xu J, Ruan H W, Liu Y, et al. Focusing light through scattering media by transmission matrix inversion[J]. Optics Express, 2017, 25(22): 27234-27246.
[58] Lee K, Park Y. Exploiting the speckle-correlation scattering matrix for a compact reference-free holographic image sensor[J]. Nature Communications, 2016, 7: 13359.
[59] Andreoli D, Volpe G, Popoff S, et al. Deterministic control of broadband light through a multiply scattering medium via the multispectral transmission matrix[J]. Scientific Reports, 2015, 5: 10347.
[60] Mounaix M, Andreoli D, Defienne H, et al. Spatiotemporal coherent control of light through a multiple scattering medium with the multispectral transmission matrix[J]. Physical Review Letters, 2016, 116(25): 253901.
[61] Drémeau A, Liutkus A, Martina D, et al. Reference-less measurement of the transmission matrix of a highly scattering material using a DMD and phase retrieval techniques[J]. Optics Express, 2015, 23(9): 11898-11911.
[62] N'Gom M, Lien M B, Estakhri N M, et al. Controlling light transmission through highly scattering media using semi-definite programming as a phase retrieval computation method[J]. Scientific Reports, 2017, 7(1): 2518.
[63] N'Gom M, Norris T B, Michielssen E, et al. Mode control in a multimode fiber through acquiring its transmission matrix from a reference-less optical system[J]. Optics Letters, 2018, 43(3): 419-422.
[64] Deng L, Yan J D, Elson D S, et al. Characterization of an

imaging multimode optical fiber using a digital micro-mirror device based single-beam system[J]. Optics Express, 2018, 26(14): 18436-18447.

[65] Zhao T R, Deng L, Wang W, et al. Bayes′ theorem-based binary algorithm for fast reference-less calibration of a multimode fiber[J]. Optics Express, 2018, 26(16): 20368-20378.

[66] Huang G Q, Wu D X, Luo J W, et al. Retrieving the optical transmission matrix of a multimode fiber using the extended Kalman filter[J]. Optics Express, 2020, 28(7): 9487-9500.

[67] Huang G Q, Wu D X, Luo J W, et al. Generalizing the Gerchberg-Saxton algorithm for retrieving complex optical transmission matrices[J]. Photonics Research, 2020, 9(1): 34-42.

[68] Wang Z Y, Wu D X, Huang G Q, et al. Feedback-assisted transmission matrix measurement of a multimode fiber in a referenceless system[J]. Optics Letters, 2021, 46(22): 5542-5545.

[69] Ancora D, Dominici L, Gianfrate A, et al. Speckle spatial correlations aiding optical transmission matrix retrieval: the smoothed Gerchberg-Saxton single-iteration algorithm[J]. Photonics Research, 2022, 10(10): 2349-2358.

[70] Wu D X, Luo J W, Lu Z B, et al. Two-stage matrix-assisted glare suppression at a large scale[J]. Photonics Research, 2022, 10(12): 2693-2701.

[71] Wu D X, Wang Z Y, Wang J, et al. Probabilistic phase shaping guided wavefront control of complex media with information-limited intensity measurements[J]. Laser & Photonics Reviews, 2023, 17(9): 2300110.

[72] Moon J, Cho Y C, Kang S, et al. Measuring the scattering tensor of a disordered nonlinear medium[J]. Nature Physics, 2023, 19: 1709-1718.

[73] Ni F C, Liu H G, Zheng Y L, et al. Nonlinear harmonic wave manipulation in nonlinear scattering medium via scattering-matrix method[J]. Advanced Photonics, 2023, 5(4): 046010.

[74] Borhani N, Kakkava E, Moser C, et al. Learning to see through multimode fibers[J]. Optica, 2018, 5(8): 960-966.

[75] Rahmani B, Loterie D, Konstantinou G, et al. Multimode optical fiber transmission with a deep learning network[J]. Light, Science & Applications, 2018, 7: 69.

[76] Zhang L H, Xu R C, Ye H L, et al. High definition images transmission through single multimode fiber using deep learning and simulation speckles[J]. Optics and Lasers in Engineering, 2021, 140: 106531.

[77] Zhu C Y, Chan E A, Wang Y, et al. Image reconstruction through a multimode fiber with a simple neural network architecture[J]. Scientific Reports, 2021, 11(1): 896.

[78] Tang P S, Zheng K P, Yuan W M, et al. Learning to transmit images through optical speckle of a multimode fiber with high fidelity[J]. Applied Physics Letters, 2022, 121(8): 081107.

[79] Liu Y F, Zhang Z S, Yu P P, et al. Learning-enabled recovering scattered data from twisted light transmitted through a long standard multimode fiber[J]. Applied Physics Letters, 2022, 120(13): 131101.

[80] Fan P F, Zhao T R, Su L. Deep learning the high variability and randomness inside multimode fibers[J]. Optics Express, 2019, 27(15): 20241-20258.

[81] Resisi S, Popoff S M, Bromberg Y. Image transmission through a dynamically perturbed multimode fiber by deep learning[J]. Laser & Photonics Reviews, 2021, 15(10): 2000553.

[82] Fan P F, Ruddlesden M, Wang Y F, et al. Learning enabled continuous transmission of spatially distributed information through multimode fibers[J]. Laser & Photonics Reviews, 2021, 15(4): 2000348.

[83] Turpin A, Vishniakou I, Seelig J D. Light scattering control in transmission and reflection with neural networks[J]. Optics Express, 2018, 26(23): 30911-30929.

[84] Rahmani B, Loterie D, Kakkava E, et al. Actor neural networks for the robust control of partially measured nonlinear systems showcased for image propagation through diffuse media [J]. Nature Machine Intelligence, 2020, 2: 403-410.

[85] Xiang C C, Xiao Y S, Dai Y, et al. Controlling light focusing through scattering medium with superpixel-based deep learning method[J]. Optik, 2022, 262: 169277.

[86] Wang J, Zhong G C, Wu D X, et al. Multimode fiber-based greyscale image projector enabled by neural networks with high generalization ability[J]. Optics Express, 2023, 31(3): 4839-4850.

[87] Huang S T, Wang J, Wu D X, et al. Projecting colorful images through scattering media via deep learning[J]. Optics Express, 2023, 31(22): 36745-36753.

[88] Wei X M, Jing J C, Shen Y C, et al. Harnessing a multi-dimensional fibre laser using genetic wavefront shaping[J]. Light, Science & Applications, 2020, 9: 149.

[89] Kim M, Choi Y, Yoon C, et al. Maximal energy transport through disordered media with the implementation of transmission eigenchannels[J]. Nature Photonics, 2012, 6: 581-585.

[90] Feng B Y, Guo H Y, Xie M Y, et al. NeuWS: neural wavefront shaping for guidestar-free imaging through static and dynamic scattering media[J]. Science Advances, 2023, 9(26): eadg4671.

[91] Shen Y C, Liu Y, Ma C, et al. Focusing light through biological tissue and tissue-mimicking phantoms up to 9.6 cm in thickness with digital optical phase conjugation[J]. Journal of Biomedical Optics, 2016, 21(8): 085001.

[92] Yaqoob Z, Psaltis D, Feld M S, et al. Optical phase conjugation for turbidity suppression in biological samples[J]. Nature Photonics, 2008, 2(2): 110-115.

[93] Cui M, Yang C H. Implementation of a digital optical phase conjugation system and its application to study the robustness of turbidity suppression by phase conjugation[J]. Optics Express, 2010, 18(4): 3444-3455.

[94] Hsieh C L, Pu Y, Grange R, et al. Imaging through turbid layers by scanning the phase conjugated second harmonic radiation from a nanoparticle[J]. Optics Express, 2010, 18(20): 20723-20731.

[95] Vellekoop I M, Cui M, Yang C. Digital optical phase conjugation of fluorescence in turbid tissue[J]. Applied Physics Letters, 2012, 101(8): 081108.

[96] Hillman T R, Yamauchi T, Choi W, et al. Digital optical phase conjugation for delivering two-dimensional images through turbid media[J]. Scientific Reports, 2013, 3: 1909.

[97] Liu Y, Ma C, Shen Y C, et al. Bit-efficient, sub-millisecond wavefront measurement using a lock-in camera for time-reversal based optical focusing inside scattering media[J]. Optics Letters, 2016, 41(7): 1321-1324.

[98] Hemphill A S, Shen Y C, Liu Y, et al. High-speed single-shot optical focusing through dynamic scattering media with full-phase wavefront shaping[J]. Applied Physics Letters, 2017, 111(22): 221109.

[99] Liu Y, Shen Y C, Ruan H W, et al. Time-reversed ultrasonically encoded optical focusing through highly scattering *ex vivo* human cataractous lenses[J]. Journal of Biomedical Optics, 2018, 23(1): 010501.

[100] Luo J W, Liu Y, Wu D X, et al. High-speed single-exposure time-reversed ultrasonically encoded optical focusing against dynamic scattering[J]. Science Advances, 2022, 8(50): eadd9158.

[101] Jang M, Ruan H W, Zhou H J, et al. Method for auto-alignment of digital optical phase conjugation systems based on digital propagation[J]. Optics Express, 2014, 22(12): 14054-14071.

[102] Azimipour M, Atry F, Pashaie R. Calibration of digital optical phase conjugation setups based on orthonormal rectangular

polynomials[J]. Applied Optics, 2016, 55(11): 2873-2880.
[103] Hemphill A S, Shen Y C, Hwang J, et al. High-speed alignment optimization of digital optical phase conjugation systems based on autocovariance analysis in conjunction with orthonormal rectangular polynomials[J]. Journal of Biomedical Optics, 2018, 24(3): 031004.
[104] Yu Y W, Sun C C, Liu X C, et al. Continuous amplified digital optical phase conjugator for focusing through thick, heavy scattering medium[J]. OSA Continuum, 2019, 2(3): 703-714.
[105] Mididoddi C K, Lennon R A, Li S H, et al. High-fidelity off-axis digital optical phase conjugation with transmission matrix assisted calibration[J]. Optics Express, 2020, 28(23): 34692-34705.
[106] Liang H P, Li T J, Luo J W, et al. Optical focusing inside scattering media with iterative time-reversed ultrasonically encoded near-infrared light[J]. Optics Express, 2023, 31(11): 18365-18378.
[107] McDowell E J, Cui M, Vellekoop I M, et al. Turbidity suppression from the ballistic to the diffusive regime in biological tissues using optical phase conjugation[J]. Journal of Biomedical Optics, 2010, 15(2): 025004.
[108] Lai P X, Xu X, Liu H L, et al. Reflection-mode time-reversed ultrasonically encoded optical focusing into turbid media[J]. Journal of Biomedical Optics, 2011, 16(8): 080505.
[109] Xu X, Liu H L, Wang L V. Time-reversed ultrasonically encoded optical focusing into scattering media[J]. Nature Photonics, 2011, 5(3): 154-157.
[110] Liu Y, Lai P X, Ma C, et al. Optical focusing deep inside dynamic scattering media with near-infrared time-reversed ultrasonically encoded (TRUE) light[J]. Nature Communications, 2015, 6: 5904.
[111] Jayet B, Huignard J P, Ramaz F. Optical phase conjugation in Nd∶YVO_4 for acousto-optic detection in scattering media[J]. Optics Letters, 2013, 38(8): 1256-1258.
[112] Blochet B, Bourdieu L, Gigan S. Focusing light through dynamical samples using fast continuous wavefront optimization [J]. Optics Letters, 2017, 42(23): 4994-4997.
[113] Horstmeyer R, Ruan H W, Yang C H. Guidestar-assisted wavefront-shaping methods for focusing light into biological tissue[J]. Nature Photonics, 2015, 9: 563-571.
[114] Vellekoop I M, van Putten E G, Lagendijk A, et al. Demixing light paths inside disordered metamaterials[J]. Optics Express, 2008, 16(1): 67-80.
[115] Vellekoop I M, Aegerter C M. Scattered light fluorescence microscopy: imaging through turbid layers[J]. Optics Letters, 2010, 35(8): 1245-1247.
[116] Hsieh C L, Pu Y, Grange R, et al. Digital phase conjugation of second harmonic radiation emitted by nanoparticles in turbid media[J]. Optics Express, 2010, 18(12): 12283-12290.
[117] Ruan H W, Haber T, Liu Y, et al. Focusing light inside scattering media with magnetic-particle-guided wavefront shaping [J]. Optica, 2017, 4(11): 1337-1343.
[118] Yu Z P, Huangfu J T, Zhao F Y, et al. Time-reversed magnetically controlled perturbation (TRMCP) optical focusing inside scattering media[J]. Scientific Reports, 2018, 8: 2927.
[119] Ruan H W, Jang M, Yang C. Optical focusing inside scattering media with time-reversed ultrasound microbubble encoded light [J]. Nature Communications, 2015, 6: 8968.
[120] Yang J M, Li L, Shemetov A A, et al. Focusing light inside live tissue using reversibly switchable bacterial phytochrome as a genetically encoded photochromic guide star[J]. Science Advances, 2019, 5(12): eaay1211.
[121] Ma C, Xu X, Liu Y, et al. Time-reversed adapted-perturbation (TRAP) optical focusing onto dynamic objects inside scattering media[J]. Nature Photonics, 2014, 8(12): 931-936.
[122] Zhou E H, Ruan H W, Yang C, et al. Focusing on moving targets through scattering samples[J]. Optica, 2014, 1(4): 227-232.
[123] Wang Y M, Judkewitz B, Dimarzio C A, et al. Deep-tissue focal fluorescence imaging with digitally time-reversed ultrasound-encoded light[J]. Nature Communications, 2012, 3: 928.
[124] Si K, Fiolka R, Cui M. Fluorescence imaging beyond the ballistic regime by ultrasound pulse guided digital phase conjugation[J]. Nature Photonics, 2012, 6(10): 657-661.
[125] Ruan H W, Jang M, Judkewitz B, et al. Iterative time-reversed ultrasonically encoded light focusing in backscattering mode[J]. Scientific Reports, 2014, 4: 7156.
[126] Si K, Fiolka R, Cui M. Breaking the spatial resolution barrier via iterative sound-light interaction in deep tissue microscopy[J]. Scientific Reports, 2012, 2: 748.
[127] Aizik D, Gkioulekas I, Levin A. Fluorescent wavefront shaping using incoherent iterative phase conjugation[J]. Optica, 2022, 9 (7): 746-754.
[128] Suzuki Y, Tay J W, Yang Q, et al. Continuous scanning of a time-reversed ultrasonically encoded optical focus by reflection-mode digital phase conjugation[J]. Optics Letters, 2014, 39(12): 3441-3444.
[129] Judkewitz B, Wang Y M, Horstmeyer R, et al. Speckle-scale focusing in the diffusive regime with time-reversal of variance-encoded light (TROVE) [J]. Nature Photonics, 2013, 7(4): 300-305.
[130] Kong F T, Silverman R H, Liu L P, et al. Photoacoustic-guided convergence of light through optically diffusive media[J]. Optics Letters, 2011, 36(11): 2053-2055.
[131] Caravaca-Aguirre A M, Niv E, Conkey D B, et al. Real-time resilient focusing through a bending multimode fiber[J]. Optics Express, 2013, 21(10): 12881-12887.
[132] Lai P X, Wang L D, Tay J W, et al. Photoacoustically guided wavefront shaping for enhanced optical focusing in scattering media[J]. Nature Photonics, 2015, 9(2): 126-132.
[133] Inzunza-Ibarra M A, Premillieu E, Grünsteidl C, et al. Sub-acoustic resolution optical focusing through scattering using photoacoustic fluctuation guided wavefront shaping[J]. Optics Express, 2020, 28(7): 9823-9832.
[134] Chaigne T, Katz O, Boccara A C, et al. Controlling light in scattering media non-invasively using the photoacoustic transmission matrix[J]. Nature Photonics, 2014, 8: 58-64.
[135] Zhao T R, Ourselin S, Vercauteren T, et al. High-speed photoacoustic-guided wavefront shaping for focusing light in scattering media[J]. Optics Letters, 2021, 46(5): 1165-1168.
[136] Luo J W, Wu D X, Liu Y, et al. Single-exposure ultrasound-modulated optical tomography with a quaternary phase encoded mask[J]. Optics Letters, 2023, 48(11): 2857-2860.

Wavefront Shaping Methods for Scattering Light Field Regulation and Its Imaging Application (Invited)

Shen Yuecheng[1], Luo Jiawei[2], Zhang Zhiling[1], Zhang Shian[1,3,4*]

[1]*State Key Laboratory of Precision Spectroscopy, East China Normal University, Shanghai* 200241, *China*;
[2]*School of Electronics and Information Technology, Sun Yat-Sen University, Guangzhou* 510006, *Guangdong, China*;
[3]*Collaborative Innovation Center of Extreme Optics, Shanxi University, Taiyuan* 030006, *Shanxi, China*;
[4]*Joint Research Center of Light Manipulation Science and Photonic Integrated Chip of East China Normal University and Shandong Normal University, State Key Laboratory of Precision Spectroscopy, East China Normal University, Shanghai* 200241, *China*

Abstract

Significance In biomedical imaging applications, optical scattering disrupts the predictability of the light path, challenging the achievement of high-resolution optical imaging in deep tissue. Even state-of-the-art microscopy is limited to operating at roughly one millimeter in depth using visible light. Overcoming the scattering effect for deep tissue imaging remains a significant challenge. Wavefront shaping methods present a promising solution, allowing researchers to achieve high-resolution imaging through scattering media. By modulating the phase of incident light and compensating for wavefront distortion due to scattering, these methods effectively refocus scattered light, enabling high-resolution imaging in deep tissue.

Wavefront shaping methods can be categorized into three types: feedback-based, transmission matrix-based, and optical phase conjugation-based. These methods differ in system complexity and time effectiveness for obtaining the phase map. Feedback-based wavefront shaping, the first successful method for focusing light through scattering media, has a simple setup and low algorithm complexity. Research in this area has focused on improving optimization algorithms to find the optimal phase distribution, enhancing robustness and convergence speed. Transmission matrix-based wavefront shaping models light propagation in a scattering medium by using a linear transmission matrix, enabling wide-field imaging of hidden objects after obtaining the optical transmission matrix. Neural networks excel in manipulating nonlinear scattering and assist in wavefront shaping, particularly in scenarios involving multimode gain fibers and strongly absorbing tissue. Optical phase conjugation-based wavefront shaping is the most efficient method, requiring only a one-time measurement to determine a row vector of the transmission matrix. It efficiently acquires and controls information about the scattered light field, demonstrating advantages in dynamic scattering processes. In applications such as imaging living tissue, where optical scattering is dynamic on a millisecond to microsecond timescale due to physiological processes, optical phase conjugation-based wavefront shaping stands out as a promising method for high-resolution imaging.

To achieve internal focusing and imaging within scattering media, wavefront shaping methods need to be combined with guiding stars. Guiding stars within the scattering medium result from local interactions with scattered light, causing observable changes in intensity, phase, and frequency. Wavefront shaping locates guiding stars by perceiving these changes, guiding scattered light to achieve focus at the guiding star's location. Focused ultrasound serves as a "virtual guiding star", freely adjustable within biological tissue. This allows researchers, under the influence of optical scattering, to achieve a bright optical focus guided by focused ultrasound. Scanning this focus and measuring the intensity of frequency-shifted light enable the reconstruction of absorption distribution images of objects within the scattering medium.

In summary, wavefront shaping methods offer new possibilities for achieving high-resolution imaging through scattering media. By modulating the incident light phase and compensating for wavefront distortion, these methods efficiently refocus scattered light for high-resolution imaging in deep tissue. Combining wavefront shaping with guiding stars holds promise for internal focusing and imaging within scattering media, particularly in biomedical imaging applications.

Progress For the first time, a research group at the University of Twente introduced the wavefront shaping method (Fig. 2). They utilized feedback-based wavefront shaping to refocus scattered light by adjusting the target function, successfully achieving simultaneous focusing of scattered light at multiple target positions (Fig. 4). Another research group then employed a coaxial interference method to obtain the optical transmission matrix of scattering media. With the acquired transmission matrix, they could focus light to arbitrary positions on the output plane (Fig. 7). To mitigate coherent noise caused by the external reference beam, direct intensity detection approaches for retrieving the transmission matrix

were proposed and validated. The optical phase conjugation-based wavefront shaping method stood out as the most efficient approach for focusing light through scattering media, relying on the time-reversal symmetry of the optical wave propagation equation.

In 2008, researchers used a phase conjugate mirror based on photorefractive crystals to focus scattered light through biological tissue. Although phase conjugate mirrors based on photorefractive crystals have advantages in processing speed and controlling mode count, their limited efficiency in generating conjugate wavefronts restricts their applicability. Consequently, the combination of high-performance cameras and spatial light modulators (SLMs) has gradually become the mainstream solution (Fig. 10). Digital optical phase conjugate mirrors have an advantage in modulation efficiency and wavelength insensitivity, establishing their dominance in optical imaging, control, and therapeutic applications.

In 2011, ultrasonic guided stars were first proposed and applied in optical phase conjugation-based wavefront shaping, successfully achieving optical focusing and imaging within scattering media. Two independent research groups in the United States demonstrated focusing light deep inside scattering media with ultrasonic guided stars (Fig. 12). In summary, the development of small-sized, high-contrast, non-invasive, and easily controllable guiding stars has become a current focus in wavefront shaping research.

Conclusions and Prospects Wavefront shaping offers an effective approach for comprehensive exploration and precise control of scattered light. This capability allows for the alleviation of information disorder caused by scattering, facilitating high-resolution optical imaging within scattering media. This review delves into the historical development of wavefront shaping, discusses various wavefront shaping methods, highlights their applications in overcoming optical scattering for deep tissue imaging, and provides insights into future trends in the advancement of wavefront shaping techniques.

Key words wavefront shaping; scattering medium; optical phase conjugation; transmission matrix; optical imaging; guiding star